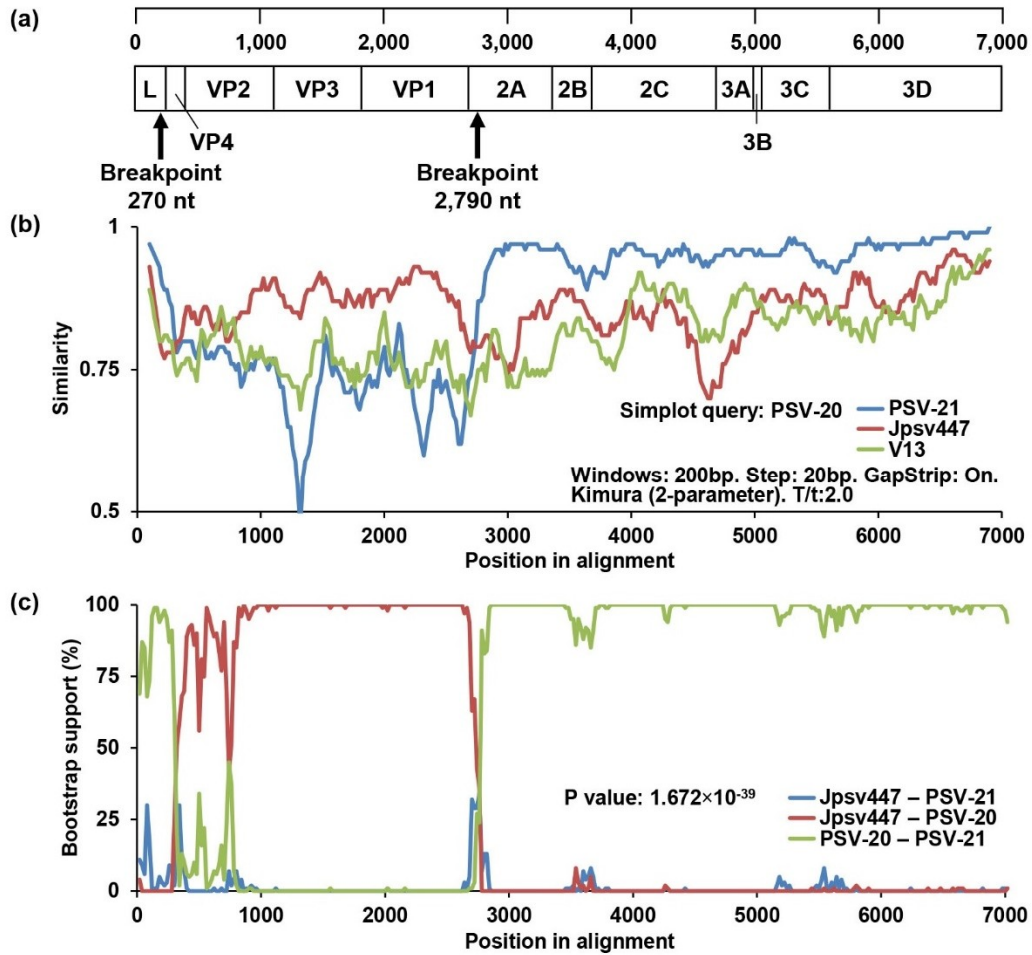


**Figure S1.** Microscopic images of Vero E6 (a-d) and BHK (e-i) cells. Mock-infected cells (a and e) and PSV-infected cells (b-d and f-i) were observed at 24 h post-infection. The cells infected with PSV-21-V (b), PSV-23-V (c), PSV-46-V (d), PSV-21-B (f), PSV-22-B (g), PSV-23-B (h) and PSV-46-B (i) showed cytopathic effects. Scale bars represent 200  $\mu\text{m}$ .

PSV-20	272	AVQDSSTYYPGT	- - - -	QAGPFYPA	TQT	294
PSV-21	272	ARLDSSQYFP	- - - - -	- - - - -	AEQL	285
PSV-22	272	ARLDSSQYFP	- - - - -	- - - - -	AEQL	285
PSV-23	272	ARLDSSQYFP	- - - - -	- - - - -	AEQL	285
PSV-26	272	AVQDSSTYYPGT	- - - -	QAG-FYS	AEQL	293
PSV-46	272	AVQDSSTYYP	- - - - -	- - - - -	AQQL	285
HuN1	272	AREDSRYYPAT	- - - -	QAG-FYPA	AEQL	293
HuN2	272	AVQDSSTYYPAT	- - - -	QIG-FYSA	AEQL	293
HuN3	272	AVQDSSTYYPAT	- - - -	QAG-FYSA	AEQL	293
HuN4	272	AVQDSSTYYPAT	- - - -	QAGLFYPA	AIQL	294
HuN9	272	AVQDSRYYFQA	- - - - -	- - - - -	SEQL	286
HuN12	272	ARLDSSQYFP	- - - - -	- - - - -	AQQL	285
HuN17	272	AREDSRYYPAT	- - - -	QTG-FYPA	AEQL	293
HuN21	272	AREDSRYYPAT	STAE	QLGPFQQ	ATQL	298
HuN23	272	AVQDSSTYYPAT	- - - -	QAG-FYPA	KQL	293
HuN27	272	AREDSRYYPAT	- - - -	QAG-FYPA	AEQL	293
HuN32	272	AREDSRYYPAT	STAE	QLGPFQQ	ATQL	298
QT2013	272	AREDSRYYPAT	- - - -	QTG-FYPA	AIQT	293
KS04105	272	AREDSRYYP	- - - - -	- - - - -	AEQL	285
KS05151	272	AREDSRYYPAT	- - - -	QTG-FYLA	AEQL	293
Jpsv447	272	AVQDSSTYYPAA	- - - -	QAG-FYPA	AEQL	293
IA33375	272	AREDSRYYPAT	- - - -	QTG-FYPA	AEQL	293
ISU-SHIC	272	ARMDSSQYFP	- - - - -	- - - - -	AEQM	285
L00798-K11 14-02	272	AVQDSRYYQA	- - - - -	- - - - -	GEQL	286
OPY-1	272	AVQDSSTYYPAT	- - - -	QAG-YYPA	TQT	293
C-6	272	AREDSMYYP	- - - - -	- - - - -	ATQT	285
V13	272	ARQDSMYYP	- - - - -	- - - - -	ATQT	285

**Figure S2.** Amino acid alignment of the VP1 C-terminal region. The deduced amino acid sequence of the VP1 C-terminal regions of Zambian PSVs and representative PSVs were aligned. The alignment of position 272-end of the C-terminal VP1 sequences is indicated.



**Figure S3.** Identification of the recombination events among PSV-20, PSV-21, and Jpsv447. (a) Predicted recombination breakpoints are shown with black arrows on the schematic diagram of the PSV genome. (b) Similarity analyses of complete ORF nucleotide sequences of PSV-20, PSV-21, Jpsv447, and V13 strains were performed using SimPlot software version 3.5.1 with the default setting. The genome of PSV-20 was used as a query sequence. The similarities plots of PSV-21 (blue line), Jpsv447 (red line), and V13 (green line) are shown. (c) Recombination breakpoint analyses were conducted using RDP version 4.97 with the sequences of Zambian strains and reference strains. The recombination among PSV-20, PSV-21, and Jpsv447 predicted by the analyses using the Bootscan method is shown. The bootstrap support values of Jpsv447 versus PSV-21 (blue line), Jpsv447 versus PSV-20 (red line), and PSV-20 versus PSV-21 (green line) are shown.

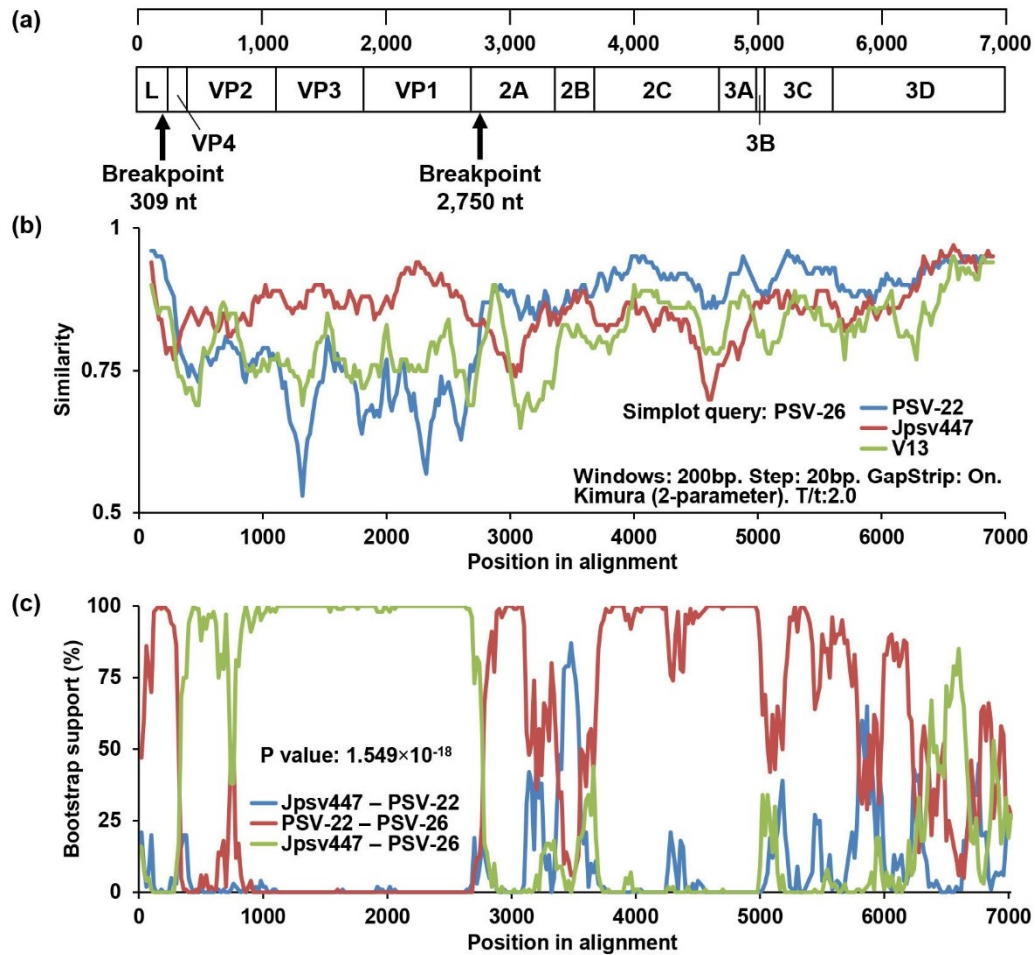


**Figure S4.** Identification of the recombination events among PSV-22, PSV-26, and Jpsv447. (a) Predicted recombination breakpoints are shown with black arrows on the schematic diagram of the PSV genome. (b) Similarity analyses of complete ORF nucleotide sequences of PSV-26, PSV-22, Jpsv447, and V13 strains were performed using SimPlot software version 3.5.1 with the default setting. The genome of PSV-26 was used as a query sequence. The similarities plots of PSV-22 (blue line), Jpsv447 (red line), and V13 (green line) are shown. (c) Recombination breakpoint analyses were conducted using RDP version 4.97 with the sequences of Zambian strains and reference strains. The recombination among PSV-22, PSV-26, and Jpsv447 predicted by the analyses using the Bootscan method is shown. The bootstrap support values of Jpsv447 versus PSV-22 (blue line), PSV-22 versus PSV-26 (red line), and Jpsv447 versus PSV-26 (green line) are shown.